BMC Neuroscience

RESEARCH

Open Access

Effects of subclinical hypothyroidism during pregnancy on mtDNA methylation in the brain of rat offspring

Liangzhuo Xie[1†], Yangling Huang[1†], Xiande Ma[1], Xiaoqiu Ma[1], Jian Wang[3], Tianshu Gao[2*] and Wei Chen[1,4*]

Abstract

Objective This study aims to investigate the impact of subclinical hypothyroidism (SCH) during pregnancy on mitochondrial DNA (mtDNA) methylation in the brain tissues of rat offspring.

Materials and methods Sixteen SD rats were randomly divided into two groups: control group (CON) and SCH group. BS-seq sequencing was used to analyze mtDNA methylation levels in the offspring's brain tissues; the 2,7-dichlorofluorescin diacetate (DCFH-DA) probe method was employed to detect reactive oxygen species (ROS) levels in brain tissues; electron microscopy was utilized to observe the mitochondrial structure in the hippocampal tissues of the offspring.

Results In the analysis of differentially methylated regions (DMRs), the mitochondrial chromosome in the SCH group exhibited 23 DMRs compared to the control group. ROS levels in the brain tissues of the SCH group were significantly higher than those in the control group ($P < 0.05$). The mitochondrial structure in the hippocampus of the SCH group was less intact compared to the CON group.

Conclusion Subclinical hypothyroidism in pregnant rats may alter the mtDNA methylation pattern in the brains of their offspring, potentially affecting mitochondrial function and structure.

Keywords Subclinical hypothyroidism, Offspring, mtDNA, Methylation, Brain tissue

Introduction

Subclinical hypothyroidism (SCH) is a common thyroid disorder during pregnancy, with a prevalence of about 3–5% [1, 2]. Epidemiological studies have shown that SCH during pregnancy may adversely affect fetal brain development, increasing the risk of intellectual disabilities by up to 2.14 times [3]. Experimental studies have found that offspring of rats with SCH during pregnancy exhibit long-term memory deficits, along with reduced levels of hippocampal BDNF, increased expression of Rap1 protein, decreased expression of hippocampal proliferation-related proteins, and increased expression of apoptosis-related proteins [4–6].

†Liangzhuo Xie and Yangling Huang contributed equally to this work.

*Correspondence:
Tianshu Gao
gaotianshu67@163.com
Wei Chen
chenwei8027@163.com
[1]Liaoning University of Traditional Chinese Medicine, Shenyang City, Liaoning Province, P. R. China
[2]Department of Endocrine, Affiliated Hospital, Liaoning University of TCM, Shenyang City, Liaoning Province, P. R. China
[3]Experimental Animal Center of Liaoning, University of Traditional Chinese Medicine, Shenyang City, Liaoning Province, P. R. China
[4]The Second Affiliated Hospital of Liaoning, University of Traditional Chinese Medicine, Shenyang City, Liaoning Province, P. R. China

Mitochondria are critically important energy centers within cells, whose dysfunction not only leads to various mental disorders but is also closely linked to cognitive functions [7]. They possess their own DNA—mitochondrial DNA (mtDNA), a circular double-stranded DNA comprising 37 genes and 16,569 base pairs [8]. Mitochondria play a central role in several cellular functions, including oxidative phosphorylation, intracellular calcium balance, the cell cycle, and apoptosis [9]. Additionally, mitochondrial function is closely related to epigenetics, which regulates gene expression through chemical modifications of DNA and histones, independently of DNA sequence variations. While most research has focused on the methylation of genomic DNA, methylation of mtDNA is also associated with neurological disease [10–12], cancer [13], and non-alcoholic fatty liver disease [14], and affects oocyte maturation and early embryonic development [15]. However, no studies have yet explored the effects of SCH during pregnancy on mtDNA methylation in fetal brain tissues.

Reactive oxygen species (ROS) are primarily produced by mitochondria during cellular metabolism. Due to their strong oxidative capacity, ROS can cause cellular damage when present in high concentrations [16]. Studies have shown that hypothyroidism leads to elevated ROS levels [17–19]. Elevated ROS can oxidize intracellular DNA, resulting in the formation of 8-hydroxydeoxyguanosine (8-OHdG), which subsequently inhibits methylation at nearby sites [20]. In addition, ROS can directly replace the catalytic role of DNA methyltransferases (DNMTs), further promoting the occurrence of methylation [21].

Given the significant prevalence of SCH during pregnancy and its potential impact on offspring cognitive health, as well as the critical role of mitochondrial function and epigenetics in brain development, this study aims to assess mtDNA methylation and ROS levels in the brain tissues of offspring from SCH-affected pregnancies in rats, in order to better understand the potential mechanisms leading to impaired neurodevelopment.

Materials and methods

Animals and materials

Sixteen non-pregnant Sprague-Dawley rats (180 ± 10 g) were purchased from Beijing Huafukang Bioscience Co., Ltd.(Beijing, China), and housed at the Specific Pathogen Free (SPF) animal facility of Liaoning University of Traditional Chinese Medicine. Laboratory conditions were maintained at 22–25 °C, with 40-50% relative humidity, and a 12-hour light/dark cycle. All animals were provided with standard feed and water ad libitum. The experimental protocol was approved by the Animal Ethics Committee of Liaoning University of Traditional Chinese Medicine (project number: 21000042021093). All methods were carried out in accordance with relevant guidelines and regulations. All rats were anesthetized via intraperitoneal injection of 3% pentobarbital sodium (0.1 mL/100 g), and deep anesthesia was confirmed by verifying the absence of pain reflexes. Blood collection and surgical procedures were then performed. To ensure animal welfare, euthanasia was carried out by administering an overdose of 3% pentobarbital sodium (0.5 mL/100 g) via intraperitoneal injection.

Before the experiment began, the rats underwent one week of acclimatization. Subsequently, they were randomly divided into two groups: control group (CON, $n = 8$) and subclinical hypothyroidism group (SCH, $n = 8$). The SCH group then underwent thyroidectomy, while the control group underwent a sham operation. Postoperatively, 0.1% calcium lactate powder was added to the drinking water of all rats, making a 1% calcium lactate solution.

One month post-operatively, blood was collected from the retro-orbital plexus to measure total thyroxine (TT4) and thyroid-stimulating hormone (TSH) levels. Successful thyroidectomy in the SCH group was confirmed when TSH levels exceeded normal values and TT4 levels were below the minimal normal threshold. Thereafter, the SCH group received subcutaneous injections of l-thyroxine (0.95 μg/100 g/day) in the neck region to establish the SCH model, while the control group received an equivalent volume of saline (50 μL/100 g/day) [6]. After 10 days, blood was collected again to measure total thyroxine (TT4) and thyroid-stimulating hormone (TSH) levels. The SCH model was confirmed to be successfully established when TSH levels were above normal values and TT4 levels showed no significant difference compared to the control group.

Then all female rats were mated with normal male rats (male to female ratio = 1:2). The day when sperm was detected on the vaginal smear in the morning was designated as day 0 of pregnancy (E0). From E0 to E13, the SCH group continued daily injections of L-T4 (0.95 μg/100 g/day). Starting from E13, the dose of L-T4 was adjusted to 1.0 μg/100 g/day, continuing until parturition. After birth, recorded as postnatal day 0 (PND0). On PND7, complete brain tissue was harvested from the offspring for experiments.

Experimental drugs

L-T4 Injection: L-T4 (Sigma USA) was prepared as an injection solution at a concentration of 1.0 μg/ml using 0.9% normal saline.

Biochemical measurements

All blood samples collected from the groups were immediately centrifuged at 13,000 g for 13 min and stored at -80 °C. Serum total thyroxine (TT4) levels were measured using a rat T4 enzyme-linked immunosorbent

assay (ELISA) kit (Cloud-Clone Corp., CEA452Ge), and serum thyroid-stimulating hormone (TSH) levels were assessed using a rat TSH ELISA kit (Cloud-Clone Corp., CEA463Mu). Both measurements were conducted strictly following the procedural steps outlined in the respective kit manuals.

mtDNA extraction, bisulfite treatment, library preparation and sequencing

The extraction of mtDNA, bisulfite treatment, library preparation and data analysis of high through-put sequencing were all conducted by Seqhealth Technology Co., Ltd., Wuhan, China (http://www.seqhealth.cn).

In this study, we first used the Mitochondrial DNA Extraction Kit (Catalog No: PH1592) to extract mtDNA from the entire brain tissue according to the instructions provided. Approximately 2–3 μg of extracted mitochondrial DNA was mixed with a certain proportion of negative control (N6-methyladenine-free Lambda DNA), and then sonicated on ice using a sonicator (JY92-IIN, Xinzhi, Ningbo, Zhejiang, China) with a 20% amplitude, 5 s on/5 seconds off cycle for 5 min to fragment the DNA into 200–500 bp pieces [22]. These fragments were subsequently subjected to bisulfite treatment via the EZ DNA Methylation-Gold™ Kit (Zymo Research, Cat. No. D5005), which converts unmethylated cytosines to thymine. A DNA library was constructed using the Accel-NGS® Methyl-Seq DNA Library Kit (Swift Biosciences, Cat. No. 30024), and PCR products were enriched, quantified, and ultimately sequenced on a NovaSeq 6000 (Illumina).

Raw sequencing data were processed using SOAPnuke (version 2.0.5) [23] for quality control, which involved removing sequencing adapters, low-quality reads, reads with high N rates, and reads that were too short. The clean reads were then aligned to the reference genome using Bismark (v0.22.3). By converting reads and the reference genome to C > T and G > A, respectively, and aligning them, the best alignment combination was selected [24]. Bismark was also used to remove duplicate reads. After reference genome alignment, Bismark (v0.22.3) was used for methylation site detection, determining methylation status based on the base type at cytosine positions in the reads aligned to the reference genome. Methylation detection results from Bismark were used to conduct a binomial distribution test B(n, p) for each cytosine site, with conditions set for a sequencing depth of at least 5 and a binomial test P-value of ≤ 0.05. Differentially methylated regions (DMRs) between paired samples or groups were detected using metilene software (version 0.2-8) [25], employing a binary segmentation algorithm combined with dual statistical tests (MWU-test and 2D KS-test), with settings for a methylation difference greater than 0.1 and a P-value ≤ 0.05. After DMR detection, genomic positions of the DMRs were annotated with genomic structural information. Conduct KEGG and GO enrichment analysis on DMR-overlapping genes using the Metascape website [26].

ROS detection in brain tissue using DCFH-DA method

Entire brain tissues from the offspring of pregnant SCH rats were placed in precooled PBS to wash away blood and other contaminants. Using ophthalmic scissors, the tissues were cut into approximately 1 mm pieces, then placed back in precooled PBS for rinsing to remove the cell debris from cutting. An appropriate amount of enzyme digestion solution was added, and the tissues were digested in a 37 °C water bath for 20–30 min with intermittent shaking. The digestion was terminated with PBS, followed by filtering through a nylon mesh to remove tissue clumps and collecting the filtered cells. The cells were then centrifuged at 500 g for 10 min, the supernatant was discarded, and the pellet was washed twice with PBS to prepare a single-cell suspension. Following the instructions provided by the kit (Shanghai Biyuntian Biotechnology Co., Ltd., No. S0033S), cells were added to fresh medium containing 10 μM DCFH-DA and incubated at 37 °C for 30 min. After incubation, the cells were washed three times with PBS and lysed using a lysis buffer composed of 50% methanol and 0.1 M NaOH. The cells were then gently scraped from the culture plate and centrifuged at 4500 rpm for 5 min. Fluorescence at 488/525 nm was subsequently measured using the anthos 2010 automated microplate reader (Anthos Labtec Instruments, Austria).

Electron microscopy

To observe the ultrastructural changes of mitochondria in hippocampal neuronal cells, we transferred the brain tissue to an ice-cold dish for dissection. The tissue was then rinsed with pre-chilled 0.9% saline at 4 °C and dried with filter paper. Subsequently, hippocampal tissue was excised and fixed in electron microscopy fixative in a dark environment for 2 h. This was followed by osmium tetroxide fixation, dehydration, infiltration, and staining with uranyl acetate and lead citrate. Finally, the treated samples were embedded and sectioned into 80 nm ultrathin slices, which were examined under a transmission electron microscope to assess changes in the mitochondrial ultrastructure.

Statistical analysis

The data in this study were analyzed using R software (version 4.2.1). For comparisons between two independent samples, if the data follow a normal distribution, an independent samples t-test will be used to assess the differences between them. For data that do not follow a normal distribution, the non-parametric Mann-Whitney

Table 1 TT4 and TSH levels in different groups of rats

Group	TT4 levels one month post-surgery (ng/mL)	TSH levels one month post-surgery (pg/mL)	TT4 levels after 10 days of L-T4 injection (ng/mL)	TSH levels after 10 days of L-T4 injection (pg/mL)
CON	73.56 ± 3.12	99.48 ± 4.03	70.55 ± 4.53	104.79 ± 3.26
SCH	19.25 ± 2.25#	165.86 ± 16.80#	79.70 ± 5.88	159.19 ± 18.94#

Data shown as group mean ± s e

#$P < 0.05$ indicates statistically significant differences

Table 2 Quality Control results for mtDNA samples

Sample	Clean reads	Clean Q20(%)	Clean Q30(%)	Clean GC(%)	Effective rate(%)
CON-1	143,479,112	96.51	91.09	24.09	97.29
CON-2	133,910,886	96.33	90.65	24.15	97.18
CON-3	167,125,274	96.53	91.16	24.43	97.1
SCH-1	136,356,292	96.44	90.97	24	97.48
SCH-2	162,882,264	96.5	91.1	24.25	97.48
SCH-3	283,279,166	96.43	90.98	24.02	97.19

Sample, Sample name. Clean Reads, Number of reads after quality control. DMR-Related Results. Clean Q20(%), Proportion of bases with quality greater than Q20 in clean reads. Clean Q30(%),Proportion of bases with quality greater than Q30 in clean reads. Clean GC(%),Average content of GC bases in clean reads. Effective Rate (%),Proportion of clean reads in the total raw output reads

U test will be employed. A p-value of < 0.05 is considered statistically significant. Numerical variables are shown as mean ± s e.

Results

TT4 and TSH levels in rats

One month post-surgery, we measured the levels of TT4 and TSH in all groups of rats to confirm the establishment of the SCH model. Compared to the CON group, the SCH group exhibited significantly lower TT4 levels ($P < 0.05$) and significantly higher TSH levels ($P < 0.05$), indicating successful thyroidectomy. Ten days after L-T4 injections, compared to the CON group, the SCH group showed no difference in TT4 levels ($P > 0.05$) but significantly higher TSH levels ($P < 0.05$), confirming the successful establishment of the SCH model. (Table 1)

Quality control of mtDNA sample and distribution of methylated C bases

After extracting mtDNA from six brain tissues, quality checks were performed. All samples had Clean Q20 and Clean Q30 values exceeding 90%, with most effective rates around 97%, indicating high quality of most sequencing reads and good reliability of sequencing data (Table 2).

Methylation analysis revealed that methylated C bases in each sample were primarily distributed in the CHH sequence context, followed by CHG and CG sequence contexts, with the CHH sequence context having the highest methylation occurrence rate. (Figures 1 and 2).

Figure 1 illustrates the proportion of methylated C bases in different sequence contexts for each sample, while Fig. 2 shows the specific methylation occurrence rates of C bases in different sequence contexts for each sample.

DMR-related results

In the DMR results, compared to the CON group, the SCH group identified 23 DMRs located on the mitochondrial chromosome. Genes overlapping with these DMRs include MT-ND2, MT-ND5, MT-ND6, MT-CYB, MT-ATP6, MT-CO1, MT-CO2, and MT-CO3. These results indicate that there are significant differences in mitochondrial gene methylation patterns between the SCH group and the CON group. (Table 3)

Go and KEGG

GO and KEGG enrichment analyses were performed on DMR-overlapping genes using the Metascape website. The KEGG results showed that these genes are primarily involved in pathways such as oxidative phosphorylation and cardiac muscle contraction. The GO results indicated that these genes are related to mitochondrial function and energy metabolism. The results are shown in Figs. 3 and 4.

ROS levels

As shown in Fig. 5, compared to the CON group, the ROS levels in the SCH group were significantly increased ($P < 0.05$).

Mitochondrial structure in the hippocampus of offspring of SCH rats during pregnancy

Through the analysis of mitochondrial ultrastructure images, we observed that the mitochondrial structure in the hippocampus of offspring from the CON group was intact, with clearly visible cristae. However, in the SCH group, the mitochondrial structure appeared blurred, with unclear cristae, indicating potential damage to the mitochondrial structure. These findings suggest that mitochondrial function in the hippocampus of offspring in the SCH group may be impaired. (Fig. 6)

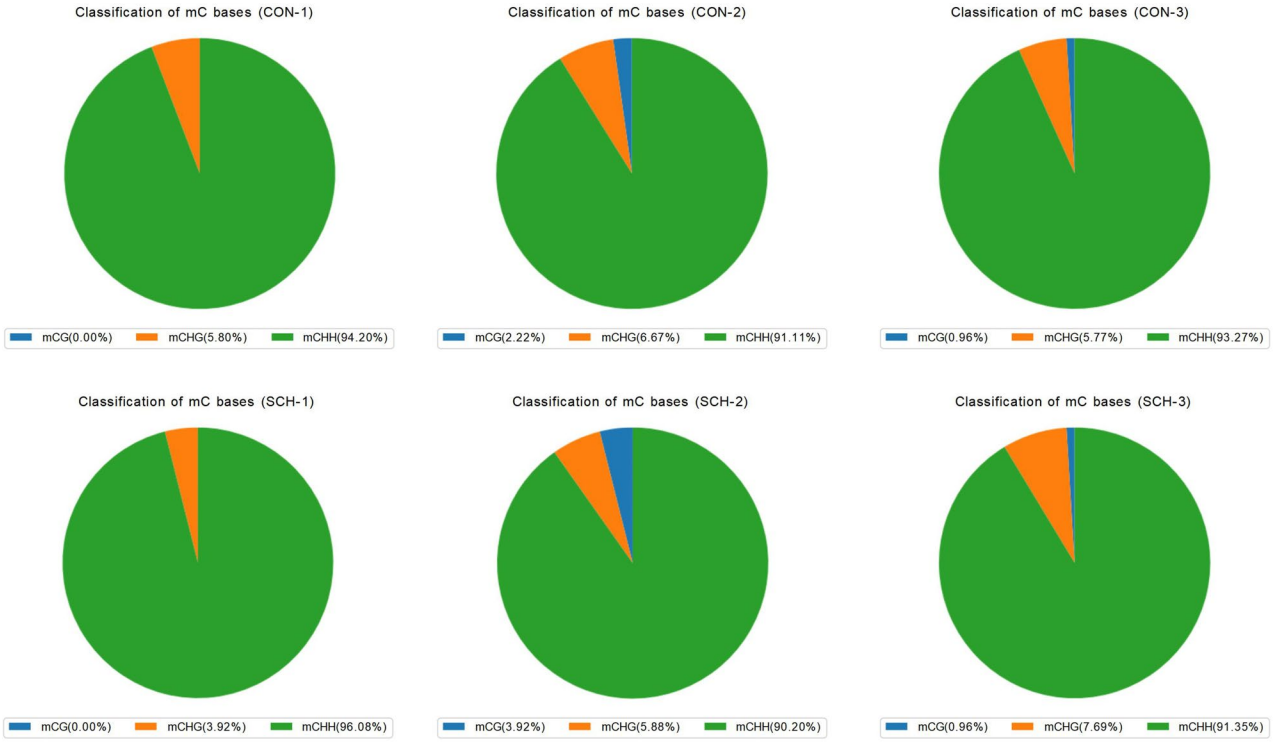

Fig. 1 Proportional distribution of methylated C bases in CG, CHG, and CHH sequence contexts

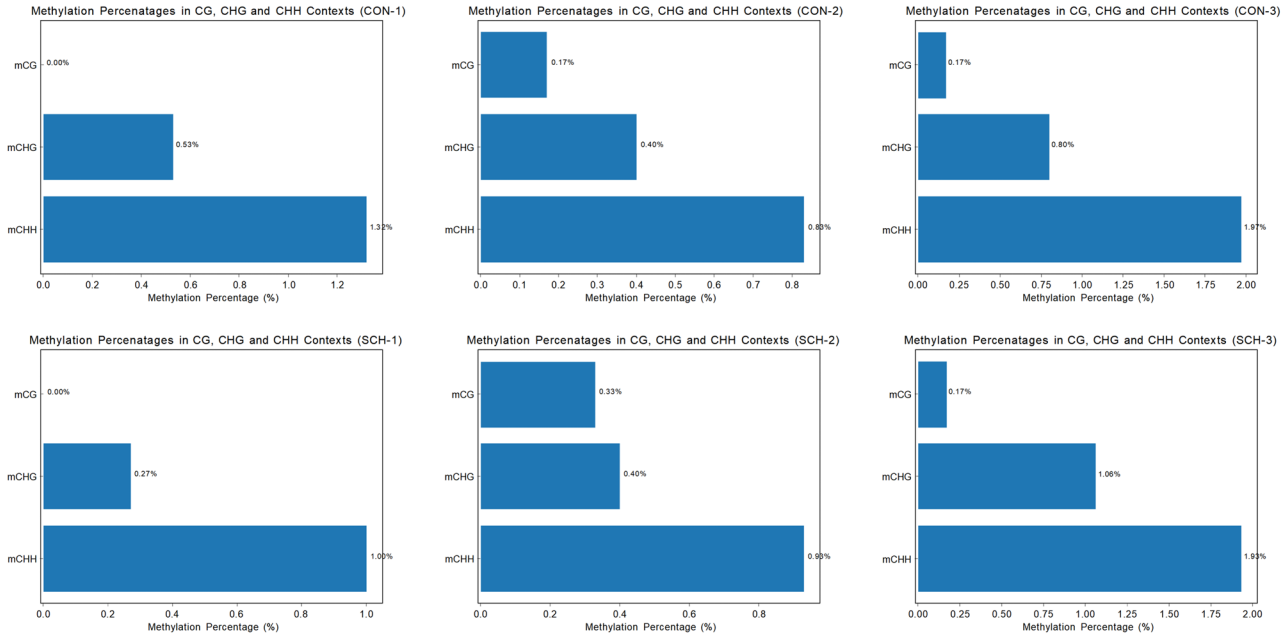

Fig. 2 Proportion of methylation occurring in CG, CHG, and CHH sequence contexts

Discussion

In this study, we identified 23 DMRs in the mtDNA of brain tissues from the offspring of rats with gestational SCH. These DMRs mapped to genes including MT-ND2, MT-ND5, MT-ND6, MT-CYB, MT-ATP6, MT-CO1, MT-CO2, and MT-CO3, and the methylation context in all rat brain tissues was mainly CHH. KEGG and GO analysis results showed that these abnormally methylated genes are primarily involved in oxidative phosphorylation (OXPHOS) and mitochondrial function. Additionally, we found that the levels of ROS were significantly elevated, and the mitochondrial structures in the hippocampus

Table 3 DMRs in Brain tissue of SCH Group offspring compared to CON Group

Chrom	Start	End	Width	Diff value	*P*-value	TranscriptID	GeneID	Context
MT	316	471	155	-0.11095	7.2787E-03	ENSRNOT00000069133; ENSRNOT00000045072	AY172581.24; AY172581.3	CG
MT	5433	5557	124	-0.11067	3.5851E-03	ENSRNOT00000050156	Mt-co1	CG
MT	14,772	14,946	174	-0.21233	4.7579E-02	ENSRNOT00000042098	Mt-cyb	CHG
MT	15,797	15,961	164	-0.11333	8.1351E-03	ENSRNOT00000044639; ENSRNOT00000049806; ENSRNOT00000051268	AY172581.2; AY172581.20; Mt-nd6	CHG
MT	510	541	31	-0.18067	2.5611E-03	ENSRNOT00000069133; ENSRNOT00000045072	AY172581.24; AY172581.3	CHH
MT	4025	4050	25	0.18333	2.9724E-02	ENSRNOT00000040993	Mt-nd2	CHH
MT	4481	4515	34	0.32867	2.3715E-04	ENSRNOT00000040993	Mt-nd2	CHH
MT	4550	4587	37	0.40361	4.0568E-04	ENSRNOT00000040993	Mt-nd2	CHH
MT	4590	4629	39	0.35476	8.9100E-05	ENSRNOT00000040993	Mt-nd2	CHH
MT	6815	6828	13	0.12500	1.6617E-02	ENSRNOT00000050156	Mt-co1	CHH
MT	7234	7255	21	-0.33767	8.8747E-03	ENSRNOT00000043693	Mt-co2	CHH
MT	7449	7495	46	0.11500	4.4996E-02	ENSRNOT00000043693	Mt-co2	CHH
MT	8167	8185	18	0.13467	9.2727E-04	ENSRNOT00000046108	Mt-atp6	CHH
MT	8418	8453	35	-0.20611	1.7426E-03	ENSRNOT00000046108	Mt-atp6	CHH
MT	8691	8722	31	-0.34733	1.0993E-02	ENSRNOT00000049683	Mt-co3	CHH
MT	11,850	11,877	27	-0.37000	2.1930E-02	ENSRNOT00000048767	Mt-nd5	CHH
MT	11,908	11,971	63	0.27200	1.7227E-03	ENSRNOT00000048767	Mt-nd5	CHH
MT	12,643	12,675	32	-0.13083	4.1503E-02	ENSRNOT00000048767	Mt-nd5	CHH
MT	12,729	12,766	37	-0.16467	1.8737E-02	ENSRNOT00000048767	Mt-nd5	CHH
MT	13,898	13,928	30	0.19167	2.6578E-02	ENSRNOT00000051268	Mt-nd6	CHH
MT	14,143	14,181	38	-0.27974	7.2916E-03	ENSRNOT00000042098	Mt-cyb	CHH
MT	14,550	14,594	44	-0.15200	1.9494E-02	ENSRNOT00000042098	Mt-cyb	CHH
MT	15,564	15,619	55	-0.16528	2.1590E-02	ENSRNOT00000044639; ENSRNOT00000049806; ENSRNOT00000051268	AY172581.2; AY172581.20; Mt-nd6	CHH

Chrom, Chromosome number. Start, DMR start position. End, DMR end position. Diff Value, The difference in average methylation levels between Group 1 and Group 2 in this DMR region (For detected methylation sites, the corresponding methylation level is calculated by mC / (mC + umC), i.e., the number of reads supporting methylation divided by the total number of reads covering the site). Pvalue, p-value. TranscriptID, Annotated transcript ID(s); if annotated to multiple transcripts, they are separated by semicolons. GeneID, Annotated gene ID(s).Context, Type of sequence environment of the methylation site, including CG, CHG, and CHH, where H represents the bases A, T, or C

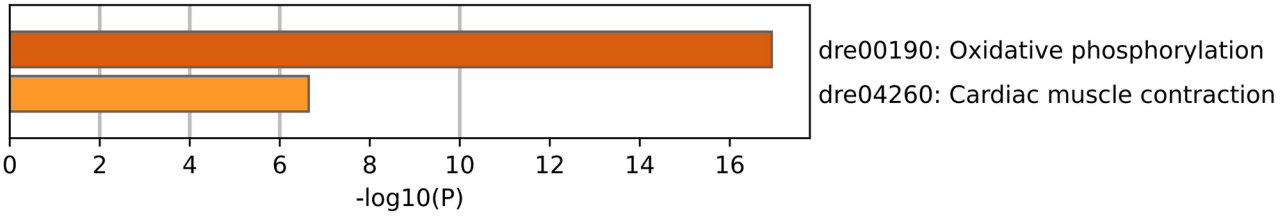

Fig. 3 KEGG pathway enrichment analysis of DMR-overlapping genes

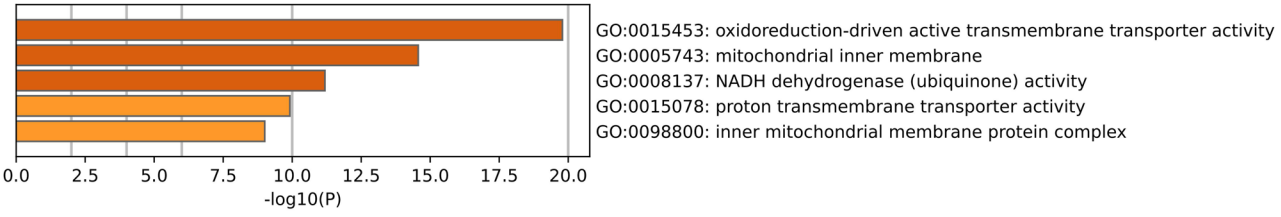

Fig. 4 GO term enrichment analysis of DMR-overlapping genes

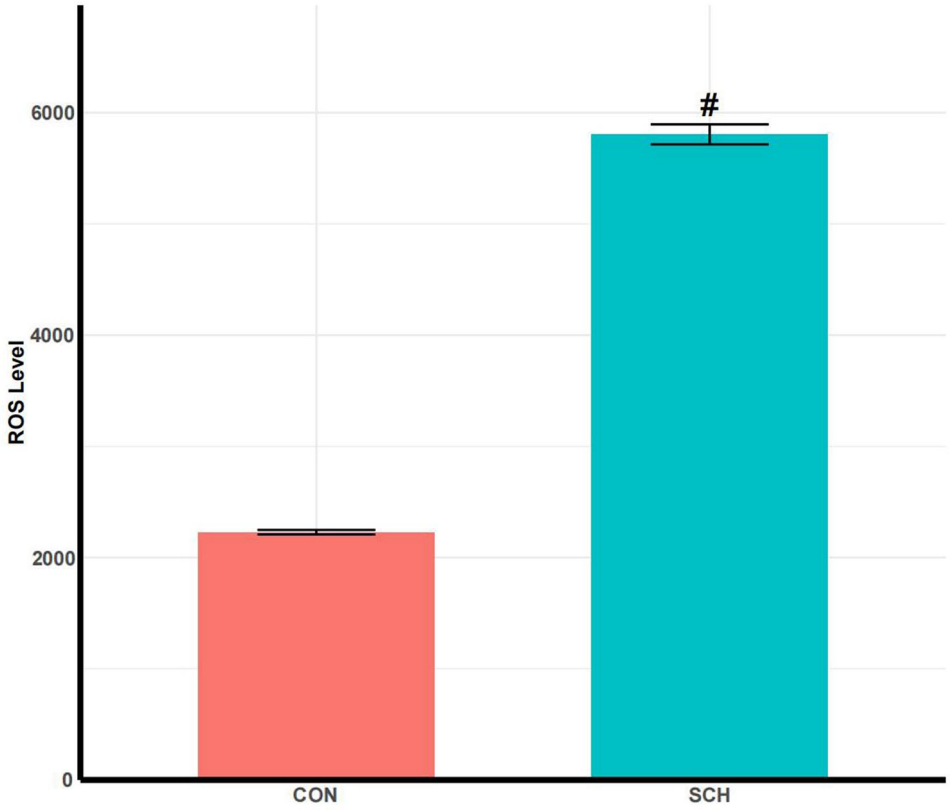

Fig. 5 ROS levels in brain tissue were measured using the fluorescent probe DCFH-DA method. Compared to the CON group, $^{\#}P < 0.05$

were damaged in the brain tissues of offspring in the model group.

Mitochondria are organelles present in all eukaryotic cells and primarily generate ATP through OXPHOS. In mitochondrial structure, folds of the inner membrane form cristae, which house protein complexes used for energy production—the electron transport chain (ETC) complexes [27]. Through OXPHOS, mitochondria generate most of the cell's required energy in the form of ATP, a process involving ETC complexes I to V [28]. The MT-ND gene family encodes protein subunits of ETC complex I, which is the first and largest enzyme in the mitochondrial respiratory chain. It plays a critical role in transferring electrons from reduced NADH to coenzyme Q10 (CoQ10) and maintaining the electrochemical gradient across the mitochondrial inner membrane [29]. MT-CYB encodes the cytochrome b subunit in ETC complex III [30]; cytochrome b receives two electrons from reduced coenzyme Q (CoQH2) and transfers them to cytochrome c [31, 32]. Complex IV is the terminal oxidase in the ETC, composed of 14 subunits, catalyzing the oxidation of cytochrome c and the reduction of molecular oxygen to water. Three of these subunits are encoded by MT-CO1 and MT-CO2, while MT-CO3 plays a role in maintaining the activity of complex IV [33]. Analysis of RNA levels of mitochondrial-encoded genes indicates that the methylation level of most mtDNA is negatively correlated with their expression levels [34]. Therefore, the overall increase in methylation levels in regions such as MT-ND2, MT-ND5, and MT-ND6 found in this study may potentially contribute to a decrease in complex I levels. Previous studies have reported an association between complex I deficiencies and neurodevelopmental abnormalities, particularly in conditions observed from late infancy to early childhood [35, 36], which may be one of the mechanisms underlying the cognitive decline in offspring of gestational SCH. Additionally, we found that the methylation level in the MT-CYB gene region decreased, which may be related to mitochondrial dysfunction in astrocytes [37].

During embryonic development in mammals, early fetal brain development relies entirely on thyroid hormones provided by the mother. In cases of gestational SCH, the mother may be unable to synthesize and secrete sufficient thyroid hormones to meet the needs of both herself and the fetus, especially during periods when fetal neural development is highly dependent on these hormones. Therefore, even if the mother's hormone levels are sufficient to maintain her own normal physiological functions, the fetus's normal development may still be affected [38]. As previously mentioned, hypothyroidism can lead to elevated levels of reactive ROS. Thus, the

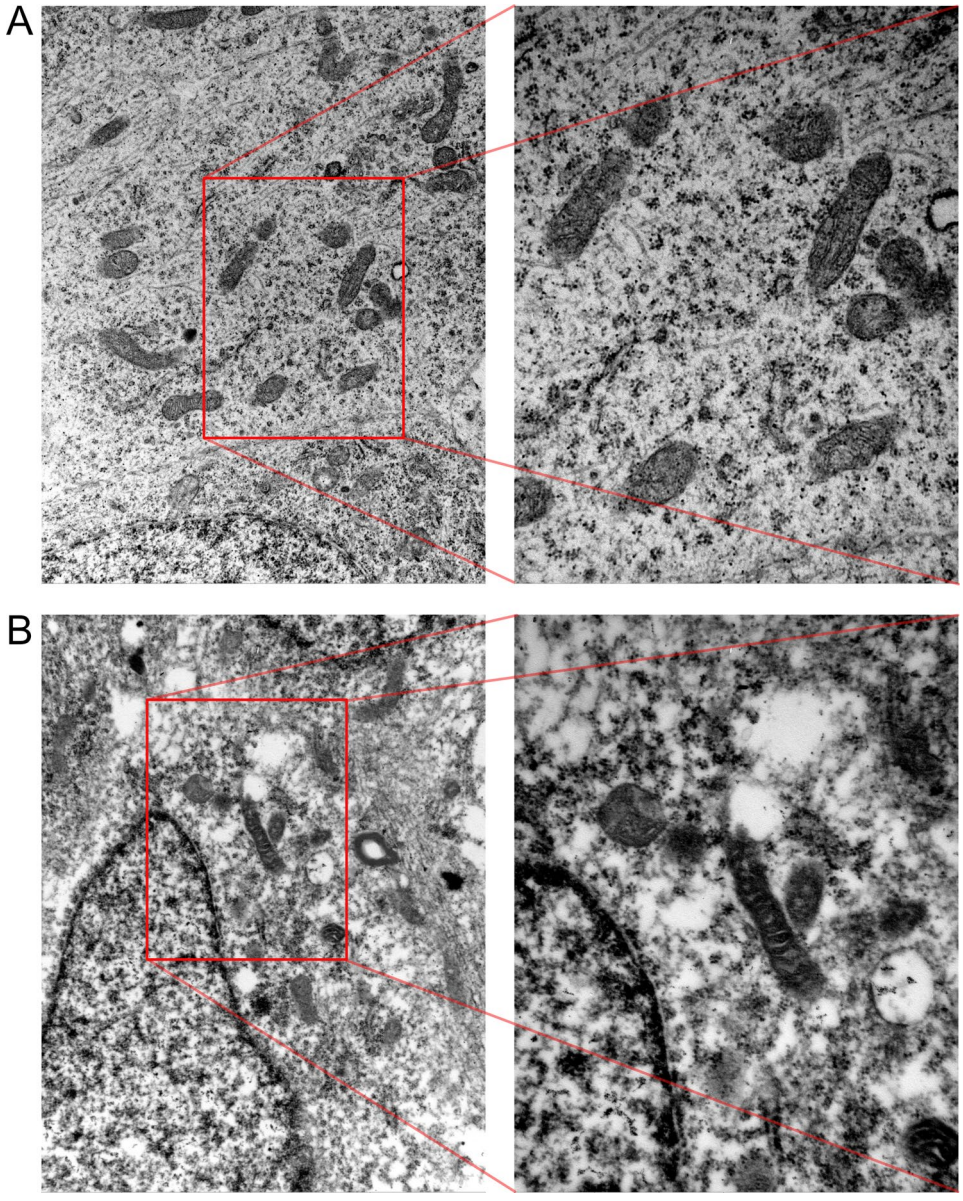

Fig. 6 Illustrates electron microscopy images of mitochondria. In Figure **A**, the CON group images are displayed, with the left panel at a magnification of 20,000x and the right panel highlighting a selected region from the left at 40,000x magnification. Similarly, Figure **B** presents the SCH group images, with the left panel at 20,000x magnification and the right panel showing a detailed region from the left at 40,000x magnification

increased ROS levels observed in the brain tissues of offspring from gestational SCH may be related to a relative deficiency of thyroid hormones in the early fetal brain tissue. ROS, as byproducts of OXPHOS, are mainly produced in mitochondria. Because mtDNA lacks introns, histones, and other protective proteins, has weak repair capabilities, and is located at the primary site of ROS generation, it is highly susceptible to oxidative damage and mutations [39, 40]. Additionally, ROS can regulate DNA methylation levels [20, 21]; therefore, the abnormal mtDNA methylation levels in the brain tissues of offspring from gestational SCH rats may be caused by elevated ROS levels.

On the other hand, mtDNA methylation may affect the electron transfer process of OXPHOS. When electrons are not fully transferred to oxygen, electron leakage may occur, interacting with oxygen to produce ROS [41]. Components such as iron-sulfur clusters and heme in the mitochondrial respiratory chain may be targets of ROS attack, leading to further impairment of mitochondrial function [41, 42]. In summary, the elevated ROS levels in the brain tissues of offspring from gestational SCH may be both initiators of mtDNA methylation and potential products of OXPHOS abnormalities, suggesting the possibility of forming a vicious cycle that further exacerbates oxidative stress in brain tissue. This significant increase

in ROS levels may be associated with a decline in fetal cognitive function, as ROS accumulation could negatively impact synaptic plasticity, thereby indirectly affecting cognitive abilities [43, 44].

Moreover, mitochondria are highly dynamic organelles whose morphology changes during different stages of the cell lifecycle; these morphological changes are important factors in determining mitochondrial function [45, 46]. Studies have shown that elevated intracellular ROS levels can alter mitochondrial morphology, potentially further affecting mitochondrial function [46]. This may partially explain the mitochondrial structural abnormalities observed in the hippocampal tissue of offspring from gestational SCH in this study.

In conclusion, this study provides new insights into the effects of gestational SCH on the brain tissue of offspring. Our research suggests that maternal SCH may affect mtDNA methylation levels in brain tissue, increase ROS levels, and cause mitochondrial structural abnormalities in the hippocampus of offspring. However, this study has several limitations. First, the relatively small sample size may limit the generalizability of the findings. Second, this study was conducted using a rodent model, which may not fully reflect the complexity of human pregnancy and fetal brain development. Additionally, although the study highlights potential mechanisms involving ROS and mtDNA methylation, direct causal relationships have not yet been established and require further experimental validation.

Future research should not only expand the sample size but also incorporate multi-omics methods such as transcriptomics and metabolomics to further explore how gestational SCH affects fetal brain development through mitochondrial pathways. Additionally, more detailed dynamic studies should be conducted on the impact of SCH at different gestational periods on offspring brain development to determine the optimal window for pregnancy management and intervention. These studies will help formulate more effective strategies for monitoring and intervening in thyroid function during pregnancy, reducing the potential negative impact of SCH on the neurodevelopment of offspring.

Acknowledgements
Thanks to the Animal Experiment Center of Liaoning University of Traditional Chinese Medicine for the technical support provided. Thanks to the National Natural Science Foundation of China for the financial support provided. Thanks to everyone who participated in this study.

Author contributions
L.X.: writing–original draft, writing–review and editing, data collection, and analysis. Y.H.: experimental design and implementation. X.M.: data analysis. X.M.: experiment optimization and data interpretation. T.G.: review and editing. J.W.: technical support and experimental design. W.C.: resources, research supervision, and review and editing.

Funding
This work was supported by National Natural Science Foundation of China (No. 82004340). WC is the project leader.

Data availability
The datasets generated and/or analysed during the current study are available in the Zenodo repository, DOI: (1) https://doi.org/10.5281/zenodo.13622850 ; (2) https://doi.org/10.5281/zenodo.13585084 .

Declarations

Ethics approval and consent to participate
All experiments were approved by the Experimental Animal Ethics Committee of Liaoning University of Traditional Chinese Medicine and adhered to the guidelines of the Institutional Animal Care and Use Committee of Liaoning University of Traditional Chinese Medicine. The SD rats used in our experiment were purchased from Beijing Huafukang Bioscience Co., Ltd. We obtained informed consent from the owners to use the animals in this study.

Consent for publication
Not applicable.

Clinical trial number
Not applicable.

Competing interests
The authors declare no competing interests.

Received: 14 August 2024 / Accepted: 22 January 2025
Published online: 24 January 2025

References

1. Shan ZY, Chen YY, Teng WP, Yu XH, Li CY, Zhou WW, et al. A study for maternal thyroid hormone deficiency during the first half of pregnancy in China. Eur J Clin Invest. 2009;39(1):37–42.
2. Teng W, Shan Z, Patil-Sisodia K, Cooper DS. Hypothyroidism in pregnancy. Lancet Diabetes Endocrinol. 2013;1(3):228–37.
3. Thompson W, Russell G, Baragwanath G, Matthews J, Vaidya B, Thompson-Coon J. Maternal thyroid hormone insufficiency during pregnancy and risk of neurodevelopmental disorders in offspring: a systematic review and meta-analysis. Clin Endocrinol (Oxf). 2018;88(4):575–84.
4. Liu D, Teng W, Shan Z, Yu X, Gao Y, Wang S, et al. The effect of maternal subclinical hypothyroidism during pregnancy on brain development in rat offspring. Thyroid. 2010;20(8):909–15.
5. Hu C, Wang S, Wu D, Yan C, Wu M. Subclinical hypothyroidism in pregnancy rats impaired offspring's spatial learning and memory and the cerebellar development. Biochem Biophys Res Commun. 2022;602:63–9.
6. Zhang F, Lin X, Liu A, Chen J, Shan Z, Teng W, et al. Maternal subclinical hypothyroidism in rats impairs spatial learning and memory in offspring by disrupting balance of the TrkA/p75(NTR) Signal Pathway. Mol Neurobiol. 2021;58(9):4237–50.
7. Buttiker P, Weissenberger S, Esch T, Anders M, Raboch J, Ptacek R, et al. Dysfunctional mitochondrial processes contribute to energy perturbations in the brain and neuropsychiatric symptoms. Front Pharmacol. 2022;13:1095923.
8. Anderson S, Bankier AT, Barrell BG, de Bruijn MH, Coulson AR, Drouin J, et al. Sequence and organization of the human mitochondrial genome. Nature. 1981;290(5806):457–65.
9. Fan LH, Wang ZB, Li QN, Meng TG, Dong MZ, Hou Y, et al. Absence of mitochondrial DNA methylation in mouse oocyte maturation, aging and early embryo development. Biochem Biophys Res Commun. 2019;513(4):912–8.
10. Chestnut BA, Chang Q, Price A, Lesuisse C, Wong M, Martin LJ. Epigenetic regulation of motor neuron cell death through DNA methylation. J Neurosci. 2011;31(46):16619–36.
11. Dzitoyeva S, Chen H, Manev H. Effect of aging on 5-hydroxymethylcytosine in brain mitochondria. Neurobiol Aging. 2012;33(12):2881–91.
12. Manev H, Dzitoyeva S, Chen H, Mitochondrial DNA. A blind spot in Neuroepigenetics. Biomol Concepts. 2012;3(2):107–15.
13. Gao J, Wen S, Zhou H, Feng S. De-methylation of displacement loop of mitochondrial DNA is associated with increased mitochondrial copy number and

nicotinamide adenine dinucleotide subunit 2 expression in colorectal cancer. Mol Med Rep. 2015;12(5):7033–8.
14. Pirola CJ, Gianotti TF, Burgueno AL, Rey-Funes M, Loidl CF, Mallardi P, et al. Epigenetic modification of liver mitochondrial DNA is associated with histological severity of nonalcoholic fatty liver disease. Gut. 2013;62(9):1356–63.
15. Piko L, Taylor KD. Amounts of mitochondrial DNA and abundance of some mitochondrial gene transcripts in early mouse embryos. Dev Biol. 1987;123(2):364–74.
16. Thannickal VJ, Fanburg BL. Reactive oxygen species in cell signaling. Am J Physiol Lung Cell Mol Physiol. 2000;279(6):L1005–28.
17. De Vito P, Incerpi S, Pedersen JZ, Luly P, Davis FB, Davis PJ. Thyroid hormones as modulators of immune activities at the cellular level. Thyroid. 2011;21(8):879–90.
18. Peixoto MS, de Vasconcelos ESA, Andrade IS, de Carvalho El Giusbi C, Coelho Faria C, Hecht F, et al. Hypothyroidism induces oxidative stress and DNA damage in breast. Endocr Relat Cancer. 2021;28(7):505–19.
19. Dos Anjos Cordeiro JM, Santos LC, de Oliveira LS, Santos BR, Santos EO, Barbosa EM, et al. Maternal hypothyroidism causes oxidative stress and endoplasmic reticulum stress in the maternal-fetal interface of rats. Free Radic Biol Med. 2022;191:24–39.
20. Valko M, Rhodes CJ, Moncol J, Izakovic M, Mazur M. Free radicals, metals and antioxidants in oxidative stress-induced cancer. Chem Biol Interact. 2006;160(1):1–40.
21. Vilkaitis G, Merkiene E, Serva S, Weinhold E, Klimasauskas S. The mechanism of DNA cytosine-5 methylation. Kinetic and mutational dissection of Hhai methyltransferase. J Biol Chem. 2001;276(24):20924–34.
22. Sun J, WH JG, Wu B, Yan S, Gao W, Lam R, et al. High quality bisulfite sequencing using nanogram amounts of genomic DNA. Int J Biochem Biotechnol. 2013;2:449–56.
23. Chen S, Zhou Y, Chen Y, Gu J. Fastp: an ultra-fast all-in-one FASTQ preprocessor. Bioinformatics. 2018;34(17):i884–90.
24. Krueger F, Andrews SR. Bismark: a flexible aligner and methylation caller for Bisulfite-Seq applications. Bioinformatics. 2011;27(11):1571–2.
25. Juhling F, Kretzmer H, Bernhart SH, Otto C, Stadler PF, Hoffmann S. Metilene: fast and sensitive calling of differentially methylated regions from bisulfite sequencing data. Genome Res. 2016;26(2):256–62.
26. Zhou Y, Zhou B, Pache L, Chang M, Khodabakhshi AH, Tanaseichuk O, et al. Metascape provides a biologist-oriented resource for the analysis of systems-level datasets. Nat Commun. 2019;10(1):1523.
27. El-Hattab AW, Scaglia F. Mitochondrial cytopathies. Cell Calcium. 2016;60(3):199–206.
28. Wallace DC. Mitochondrial diseases in man and mouse. Science. 1999;283(5407):1482–8.
29. Fassone E, Rahman S. Complex I deficiency: clinical features, biochemistry and molecular genetics. J Med Genet. 2012;49(9):578–90.
30. Berry EA, Guergova-Kuras M, Huang LS, Crofts AR. Structure and function of cytochrome bc complexes. Annu Rev Biochem. 2000;69:1005–75.
31. Brandon M, Baldi P, Wallace DC. Mitochondrial mutations in cancer. Oncogene. 2006;25(34):4647–62.
32. Fernandez-Vizarra E, Zeviani M. Mitochondrial disorders of the OXPHOS system. FEBS Lett. 2021;595(8):1062–106.
33. Sharma A, Schaefer ST, Sae-Lee C, Byun HM, Wullner U. Elevated serum mitochondrial DNA in females and lack of altered platelet mitochondrial methylation in patients with Parkinson s disease. Int J Neurosci. 2021;131(3):279–82.
34. Sirard MA. Distribution and dynamics of mitochondrial DNA methylation in oocytes, embryos and granulosa cells. Sci Rep. 2019;9(1):11937.
35. Rahman S, Blok RB, Dahl HH, Danks DM, Kirby DM, Chow CW, et al. Leigh syndrome: clinical features and biochemical and DNA abnormalities. Ann Neurol. 1996;39(3):343–51.
36. Leigh D. Subacute necrotizing encephalomyelopathy in an infant. J Neurol Neurosurg Psychiatry. 1951;14(3):216–21.
37. Doke M, Jeganathan V, McLaughlin JP, Samikkannu T. HIV-1 Tat and cocaine impact mitochondrial epigenetics: effects on DNA methylation. Epigenetics. 2021;16(9):980–99.
38. Lavado-Autric R, Auso E, Garcia-Velasco JV, Arufe Mdel C, Escobar del Rey F, Berbel P, et al. Early maternal hypothyroxinemia alters histogenesis and cerebral cortex cytoarchitecture of the progeny. J Clin Invest. 2003;111(7):1073–82.
39. Clayton DA. Transcription of the mammalian mitochondrial genome. Annu Rev Biochem. 1984;53:573–94.
40. Croteau DL, Bohr VA. Repair of oxidative damage to nuclear and mitochondrial DNA in mammalian cells. J Biol Chem. 1997;272(41):25409–12.
41. Brown GC, Borutaite V. Inhibition of mitochondrial respiratory complex I by nitric oxide, peroxynitrite and S-nitrosothiols. Biochim Biophys Acta. 2004;1658(1–2):44–9.
42. Cleeter MW, Cooper JM, Darley-Usmar VM, Moncada S, Schapira AH. Reversible inhibition of cytochrome c oxidase, the terminal enzyme of the mitochondrial respiratory chain, by nitric oxide. Implications for neurodegenerative diseases. FEBS Lett. 1994;345(1):50–4.
43. Kishida KT, Klann E. Sources and targets of reactive oxygen species in synaptic plasticity and memory. Antioxid Redox Signal. 2007;9(2):233–44.
44. Sesti F, Liu S, Cai SQ. Oxidation of potassium channels by ROS: a general mechanism of aging and neurodegeneration? Trends Cell Biol. 2010;20(1):45–51.
45. Youle RJ, van der Bliek AM. Mitochondrial fission, fusion, and stress. Science. 2012;337(6098):1062–5.
46. Ahmad T, Aggarwal K, Pattnaik B, Mukherjee S, Sethi T, Tiwari BK, et al. Computational classification of mitochondrial shapes reflects stress and redox state. Cell Death Dis. 2013;4(1):e461.

Publisher's note